SAND--79-2379

DE82 003079

SAND79-2379
Unlimited Release
Printed October 1981

GAS-DRIVEN FRACTURE PROPAGATION

R. H. Nilson
Sandia National Laboratories
Albuquerque, New Mexico 87185

ABSTRACT

A one-dimensional gas-flow drives a wedge-shaped fracture into a linearly elastic, impermeable half-space which is in uniform compression, σ_∞, at infinity. Under a constant driving pressure, p_o, the fracture/flow system accelerates through a sequence of three self-similar asymptotic regimes (laminar, turbulent, inviscid) in which the fracture grows like an elementary function of time (exponential, near-unity power, and linear; respectively). In each regime, the transport equations are reducible under a separation-of-variables transformation. The integro-differential equations which describe the viscous flows are solved by iterative shooting-methods, using expansion techniques to accommodate a zero-pressure singularity at the leading edge of the flow. These numerical results are complemented by an asymptotic analysis for large pressure ratio ($N = p_o/\sigma_\infty \to \infty$) which exploits the disparity between the fracture-length and penetration-length of the flow. The considered prototypic problem has geologic applications: containment evaluation of underground nuclear tests, explosive stimulation of oil and gas wells, and explosive permeability-enhancement prior to in-situ combustion of coal or oil-shale.

TABLE OF CONTENTS

LIST OF FIGURES

LIST OF TABLES

NOMENCLATURE

N, Re	Pressure ratio: $N = p_o/$ [illegible], Reynolds number: $Re = uw_0/$[illegible]
[illegible]	Shear modulus, Poisson's ratio, octonic stress
a, b,	Constants in turbulence model
c_o, [illegible]	Sound speed, specific heat [illegible], viscosity
t, t_o, [illegible]	Time (dimensional, t_o = [illegible] = $t_c/$[illegible])
x, [illegible]	Position (dimensional, [illegible])
[illegible], ℓ_o	Fracture length (ℓ = [illegible])
p, p_o, P	Pressure (dimensional, [illegible])
u, u_o, U	Velocity (dimensional, [illegible])
w, w_o, W	Aperture (dimensional, [illegible])
[illegible], ρ_o, ρ	Density (dimensional, [illegible])
f, q	Growth rate (fracture [illegible])
[illegible]	Separation constant (gene[illegible])
[illegible]	Entry-layer thickness [illegible]

I. INTRODUCTION

In a fluid-driven fracture process, it is the internal fluid pressure which wedges open the fracture and, hence, controls the rate of propagation. The fluid velocity and the induced fracture-tip velocity are generally small compared to the velocity of stress waves; so, the displacement field adjusts almost instantaneously to the changing fluid-pressure distribution. This quasi-steady strain field is representative of both the classical pump-driven hydrofracture and of the late time response of explosion-driven systems. Despite this similarity in the solid mechanics of these two cases, there is very little similarity in the fluid mechanics:

(1) Liquid-driven hydrofracture of petroleum reservoirs is a well-developed practice [1]. Here the fracture-velocity is controlled by a predetermined pumping schedule, and the injected fluid is incompressible. The flow-field and the elastic-field are both quasi-steady. The driving pressure is only slightly greater than the confining tectonic stress, and the fluid pressure is nearly uniform along the fracture.

(2) Gas-driven fracture propagation arises in a number of current or proposed applications: containment of underground nuclear tests; explosive stimulation of oil, gas, and geothermal wells; permeability enhancement of oil shale or coal prior to in-situ combustion. Here the fracture velocity is controlled by the dynamic interaction of a compressible fluid with the elastic

solid. Only the elastic-field is quasi-steady. The driving pressure, p_o, may greatly exceed the resisting compressive stress, σ_∞, and the fluid pressure varies considerably along the fracture.

The latter problem is addressed in the present paper and in two previous studies [2,3].

In those previous analyses of gas-driven fracture, the conservation equations are integrated in space and time using general numerical methods which are applicable to complex geometries, to porous media, and even to multiphase flows. Although very general and informative in these regards, the previous studies suppress the fluid/solid coupling by neglecting temporal wall-divergence in the flow analysis and also by imposing an arbitrary pressure at [3] or near [2] the tip, rather than enforcing continuity and a local specification of the stress state. These coupling considerations may be of little consequence when the pressure ratio $N = p_o/\sigma_\infty$ is near unity, but with increasing N, they become the dominant determinant of even the qualitative behavior.

The present study addresses the elementary problem of a wedge-shaped, gas-driven fracture in a linearly elastic, impermeable medium. Under constant driving pressure, the flow accelerates through a sequence of self-similar, asymptotic regimes (laminar, turbulent, and inviscid) in which the conservation equations are separable, time from position. The resulting ordinary differential equations are solved, for the laminar and turbulent regimes, using standard shooting methods. The analysis reveals a number of interesting mathematical and physical features which are summarized at

the end of the paper. The results are useful in estimating fracture growth rates under subsonic gas-drive.

II. FORMULATION

In the planar geometry of Figure 1, a constant pressure p_o drives a wedge-shaped fracture to a penetration depth $\ell(t)$. The internal gas pressure $p(x,t)$ spreads the walls of the fracture, producing a flow channel with aperture width, $w(x,t)$. The considered geometry is often studied in oil-field applications where vertical-plane fractures are expected to occur because the least-principle-stress is horizontal. Although there are three-dimensional cases where the fracture-height (here assumed infinite) influences the aperture [4,5], the present wedge-shaped configuration is submitted as a simple and representative case.† This wedge-shaped example should place an upper bound on fracture growth because it neglects the fracture-closing effect of a finite fracture-height and because it eliminates the flow-divergence which occurs in axisymmetric penny-shaped configurations.

Since the velocity of stress waves greatly exceeds the fracture velocity in a subsonic gas-drive, the displacement field adjusts almost instantaneously to the changing pressure loading. A quasi-steady stress analysis is therefore appropriate. Suppose that the tectonic stress σ_∞ (normal to the fracture plane) is uniform in the far field, that $x = 0$ is a line of symmetry, and that viscous traction is negligible. Then the aperture distribution is functionally related to the pressure distribution by the theory of linear elasticity [5,6,7].

---

†The radial growth of a penny-shaped crack is also described by the wedge-shaped analysis, so long as the penetration depth (ℓ_R) is small compared to the base radius (R_o), as in the early-time propagation of a fracture from an underground nuclear cavity.

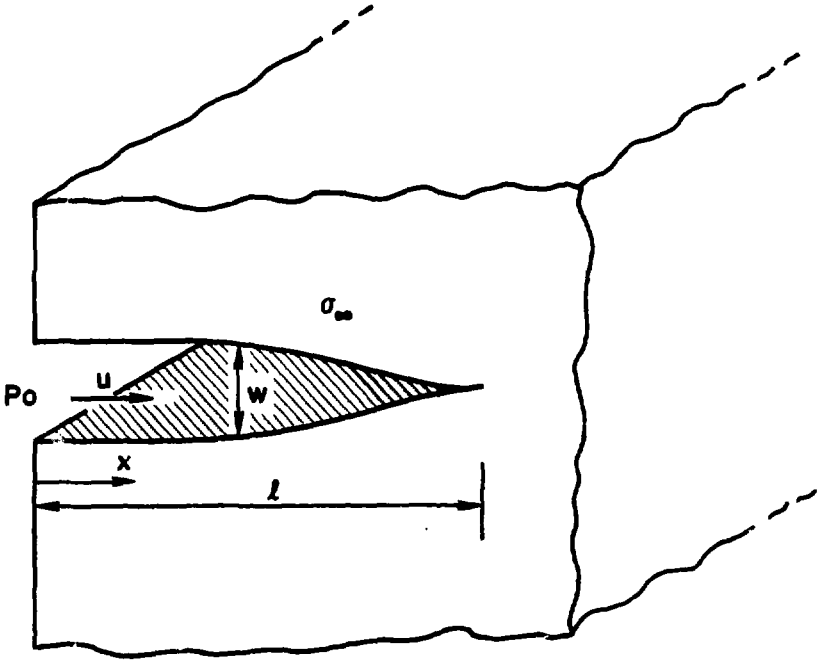

FIGURE 1. Schematic of Wedge-Shaped Fracture Driven by Internal Gas Pressure

$$w(\theta,t) = \frac{4(1-\nu)\ell}{\pi G}\int_{\theta}^{1}\int_{0}^{\sigma}\frac{[p(\zeta)-\sigma_{\infty}]d\zeta}{\sqrt{\sigma^2-\zeta^2}}\frac{\sigma d\sigma}{\sqrt{\sigma^2-\theta^2}} \qquad (1)$$

G and ν are the shear modulus and Poisson's ratio, respectively, and $\theta = x/\ell(t)$ is the normalized position variable. Since $w(\theta,t)$ depends on t only through $\ell(t)$, the shape $w(\theta)$ is preserved during fracture growth whenever $p(\theta)$ remains stationary.

The mechanics of the tip region are addressed by Barenblatt's theory of equilibrium fracture [8] which has been broadly applied [5,7,8,9] to geologic hydrofracture. The theory postulates that the stress must be finite at the tip of a fracture which is in mobile equilibrium. Accordingly, the pressure must satisfy an integral constraint [7,8]

$$\int_{0}^{1}\frac{[p(\theta)-\sigma_{\infty}]}{\sqrt{1-\theta^2}}d\theta = \frac{K}{\sqrt{2\ell}}\ , \qquad (2)$$

which ensures a smooth closure with $w_x = \partial w/\partial x = 0$, rather than a cusp at the tip. Although this argument removes the indefiniteness of the fracture length, it raises the question of tensile strength (or cohesive modulus [7,8], or stress intensity factor [9]), as embodied in the symbol K immediately above. Fortunately, estimates show [8,10] that the tensile strength often has a negligible influence in the geologic applications where the resistive (fracture closing) effect of the in-situ compressive stress is far greater than the local action of molecular cohesion. This is particularly true when fractures are long and when natural fissuring is taken into account. The tensile strength is therefore neglected by setting K = 0.

In scaling the equations it is helpful to examine the limiting case where the driving pressure greatly exceeds the tectonic stress

$$N \equiv \frac{p_o}{\sigma_\infty} >> 1 \quad . \tag{3}$$

The Barenblatt condition (2) then demands a steep pressure decline within a narrow entry-zone (i.e., boundary-layer) just inside the entrance. Under the rough approximation that the pressure decreases linearly to zero in crossing this boundary-layer, the elastic solution (1,2) furnishes the following a priori estimates of the boundary-layer thickness $\tilde{\delta}$ and the entrance aperture $\tilde{w}(0)$

$$\begin{aligned} \tilde{\delta} &\simeq \ell \frac{\pi}{N} + O\left(\frac{\tilde{\delta}}{\ell}\right)^3 \\ \tilde{w}(0) &\simeq \frac{4(1-\nu)p_o}{\pi G} \ell \frac{\pi}{2N} \ell n \left(\frac{2\sqrt{e}\, N}{\pi}\right) + O\left(\frac{\tilde{\delta}}{\ell}\right)^3 , \end{aligned} \tag{4}$$

These expressions are useful in scaling the problem, and they are shown to be asymptotically exact for a laminar flow as $N \to \infty$.

Transient compressible flow in the fracture is governed by conservation of mass and momentum, here written in the one-dimensional form [11]

$$\begin{aligned} &\frac{\partial}{\partial t}(\rho w) + \frac{\partial}{\partial x}(\rho w u) = 0 \\ &\frac{\partial}{\partial t}\left(\rho w u\right) + \frac{\partial}{\partial x}\left(\rho w u^2\right) = -\rho w\left(\frac{1}{\rho}\frac{\partial p}{\partial x} + \lambda\right) , \end{aligned} \tag{5}$$

in which ρ and u are density and velocity, each averaged across the channel [12]. The viscous shear stress λ is approximated as

follows for the limiting cases of low and high Reynolds number ($Re_o = u_o w_o \rho_o / \mu_o$), respectively

$$\lambda \equiv \frac{2\tau_w}{\rho w} = \frac{1}{\rho}\frac{12\mu u}{w^2} \qquad \text{(laminar)}$$
$$= a\left(\frac{\varepsilon}{w}\right)^b \frac{u^2}{w} \qquad \text{(turbulent)} \; . \tag{6}$$

The former is the standard Poiseuille expression for a laminar channel flow; the latter is based on an experimental study ($a \approx 0.1$, $b \approx 0.5$) [13] of turbulent flow in simulated geologic fractures having roughness heights ε. Regarding thermodynamics, it is here assumed that the gas is both ideal and isothermal

$$\rho = \frac{p}{RT_o} \; , \quad \frac{dp}{d\rho} = RT_o = \frac{c_o^2}{\gamma} \; , \tag{7}$$

which depicts a convenient and representative limiting case, and often places an upper bound [2] on fracture growth. The opposite extreme of adiabatic flow is equally tractable.

III. ANALYSIS

To solve the stated problem we will first apply a general separation-of-variables transformation, carrying along in parallel the distinct cases of laminar and turbulent flow. It then becomes apparent from examination of the resulting ordinary differential equations (ODE's) that the fracture growth process can be partitioned into a sequence of asymptotic regimes: exponential fracture growth in the early-time laminar flow regime, power-law fracture growth in the intermediate-time turbulent flow regime, and ultimately a linear fracture growth (e.g. choked) in the late-time inertia dominated flow regime. In this section, #3, several matters are discussed: the scaling and transformations are introduced, the time-dependent ODE's are integrated, a physical explanation is given for the progressive acceleration of the fracture growth phenomenon, and preparations are made for dealing with a singularity in the flow field. The integration of the space-dependent ODE's is accomplished in sections #4 and #5, respectively, for the separate cases of laminar and turbulent flow; and the laminar/turbulent transition is discussed in section #6.

The transformation to ordinary differential equations is accomplished by a separation-of-variables approach which distinguishes between global dependence on the growth rate $\ell(t)$ and local dependence upon the normalized position variable θ. Denoting the fracture-growth function as

$$\ell(t) = \ell_o g(\tau) \quad , \tag{8}$$

the appropriate independent variables are

$$\theta = \frac{x}{\ell_o g(\tau)} \quad , \quad \tau = \frac{t}{t_o} \quad . \tag{9}$$

The dependent variables w, u, p, and ρ are now presumed separable in a manner which is compatible with the constant boundary conditions on P and ρ, and is compatible with the observation that $w(\theta,t)$ increases linearly with $\ell(t)$, and is minimally restrictive on $u(x,t)$.

$$\begin{aligned} w(x,t) &= w_o g(\tau)\, W(\theta) & \qquad p(x,t) &= p_o P(\theta) \\ u(x,t) &= u_o f(\tau)\, U(\theta) & \qquad \rho(x,t) &= \rho_o \rho(\theta) \end{aligned} \tag{10}$$

in which ℓ_o, u_o, t_o, p_o and ρ_o are characteristic constants; f and g are functions of τ alone; P, ρ, W and U depend upon both x and τ, but only through $\theta(x,\tau)$. Thus, the PDE's (5,6) can be transformed into a separable form by substituting the separated expressions for the dependent variables (10) into the PDE's (5,6) and then expanding the derivatives as follows

$$\frac{\partial}{\partial x} = \frac{1}{\ell_o g(\tau)} \frac{\partial}{\partial \theta}, \quad \frac{\partial}{\partial t} = \frac{1}{t_o} \left(\frac{\partial}{\partial \tau} - \theta \frac{1}{g} \frac{\partial g}{\partial \tau} \frac{\partial}{\partial \theta} \right)$$

Then, letting

$$t_o \quad \frac{\ell_o}{u_o} \quad , \quad \frac{w_o}{\ell_o} = \left[\frac{4(1-\nu)}{\pi} \frac{P_o}{G} \right] \frac{\pi}{2N} \ell n \left(\frac{2\sqrt{e}\, N}{\pi} \right) , \tag{11}$$

the latter from (4b), and noting that $\rho(\theta) = P(\theta)$ in isothermal flow, the problem statement (5,6,1) becomes

$$\theta WP' - \frac{f}{g}(WPU)' = P\,(W - \theta W') \tag{12}$$

$$\gamma\left(\frac{u_o}{c_o}\right)^2\left\{f'gU - \theta fg'U' + f^2UU'\right\} + \frac{1}{P}P' = -\frac{u_o}{u_\ell}\frac{f}{g}\frac{U}{PW^2} \quad \text{(laminar)} \tag{13}$$

$$= -\frac{u_o}{u_t}\frac{f^2}{g^b}\frac{U^2}{W^{(1+b)}} \quad \text{(turbulent)}$$

$$W = \frac{2N}{\pi\, \ln(2\sqrt{\epsilon}\, N/\pi)}\int_\theta^1\int_0^\sigma \frac{[P(\zeta)-N^{-1}]d\zeta}{\sqrt{\sigma^2 - \zeta^2}}\,\frac{\sigma d\sigma}{\sqrt{\sigma^2 - \theta^2}} \quad . \tag{14}$$

Subject to the boundary and integral conditions (the latter from (2))

$$P(0) = 1 \quad , \quad \int_0^1 \frac{P(\theta)\, d\theta}{\sqrt{1 - \theta^2}} = \frac{\pi}{2N} \quad . \tag{15}$$

The primes on W, U and P indicate derivatives with respect to θ, whereas primes on f or g represent derivatives with respect to τ. In these equations there appear three different velocity scales: the sound speed c_o, the laminar velocity u_ℓ, and the turbulent velocity u_t, with the latter two defined in the following way

$$u_\ell = \left(\frac{w_o}{\ell_o}\right)^2 \frac{c_o^2\, \rho_o \ell_o}{12\mu_o\gamma} \quad , \quad u_t = \left[\left(\frac{w_o}{\ell_o}\right)\frac{c_o^2}{a\gamma}\left(\frac{w_o}{\epsilon}\right)^b\right]^{\frac{1}{2}} \tag{16}$$

It is hereafter assumed that the characteristic Mach number, $M_o = u_o/c_o$, is sufficiently small that the inertial terms (in script brackets) remain negligible during the time of interest. Then, the reference velocity u_o is taken as either u_ℓ or u_t, in the

laminar and tubulent cases respectively in order that there remains only one parameter, N.

The usual separation argument requires that the time functions satisfy (for small M_o) either

$$\begin{array}{lllll} & g' = \alpha_\ell f & \text{and} & g = f & \text{(laminar)} \\ \text{or} & g' = \alpha_t f & \text{and} & g^b = f^2 & \text{(turbulent)} \end{array} . \tag{17}$$

In each, only the one separation constant, α, need be left arbitrary to maintain full generality. So, by integration of (17)

$$\begin{array}{ll} g = \exp(\alpha_\ell \tau_\ell) & \text{(laminar)} \\ \text{or} & \\ g = \left(C + \frac{2-b}{2}\, \alpha_t \tau_t\right)^{2/(2-b)} & \text{(turbulent)} \end{array} \tag{18}$$

The time variable τ is subscripted here as a reminder that the time scale ($t_o = \ell_o/u_o$) is different for the laminar and turbulent periods. Since f and g are increasing with τ, the flow is accelerating from laminar dominance at early times to turbulent dominance at intermediate times, followed by inviscid inertial dominance even later. Thus, the constant of integration in g is taken as unity in the laminar case to have $\ell = \ell_o$ when $t = 0$, and in the turbulent case the constant C, which drops out at late times, is determined by matching considerations at laminar/turbulent transition.

The functional character of the fracture growth can be explained by an informal physical argument which is outlined below for a laminar flow. Taking the inlet aperture $\tilde{w}$ as representative of the entire channel, the increasing fracture volume ($V \sim \tilde{w}\ell$) must be accounted for by the inflow of gas ($\tilde{w}\tilde{u}$) which is, in turn,

controlled by molecular friction ($\tilde{u} \sim \Delta p \tilde{w}^2/\ell$)

$$\frac{d}{dt}(\tilde{w}\ell) \sim \frac{\tilde{w}^3 \Delta p}{\ell} \quad . \tag{19}$$

Since Δp is constant and $\tilde{w}$ is directly proportional to ℓ (from elasticity), the above differential equation suggests that ℓ grows exponentially. In the proposed separation-of-variables approach, the separation constant α serves as a quantitative link between this fracture growth argument and a flow-structure analysis. This analysis is based on the integro-differential equations which relate P, W and U. But first, there is need for a qualitative discussion concerning the boundary conditions at the leading edge.

The presence of high pressure in the entry region is mechanically communicated to the entire flow. Global spreading and frontal extension of the fracture walls pulls a vacuum in the tip region, drawing the flow down the channel. The influence of temporal divergence is illustrated by the following rearrangement of the continuity equation (Eqn 12 with $f/g' = 1/\alpha$ from 17a or 17b)

$$PU' + (U - \alpha\theta)P' = -P[(U - \alpha\theta)\frac{W'}{W} + \alpha] \quad , \tag{20}$$

in which $U - \alpha\theta$ is the local velocity of the fluid relative to the moving coordinate system (since $(dx/dt)_\theta/u_o f = \alpha\theta$). Whenever $U - \alpha\theta > 0$, the flow experiences the axial convergence ($W_\theta < 0$) of the wedge-shaped channel, particularly near the tip where $W'/W \to \infty$. But, there is an offsetting effect ($P\alpha$ term) due to the temporal divergence ($w_\tau > 0$) of the walls at any fixed θ and this is dominant near $\theta = 0$, where $W' \to 0$. The flow, therefore, sees a diverging-converging channel.

Evacuation of the tip region due to wall-divergence is favored by the smooth closure, and hence small aperture, within the leading zone. The resulting viscous stresses ($\sim 1/W^n$, $n = 2$, or $1 + b$) prevent the flow from overtaking the tip. An analogous situation occurs in liquid-driven fractures where the fracture-fluid is unable to wet the tip [7,8,9]. In spite of these expectations of an evacuated tip, the only justifiable a priori assertion is that no mass crosses the impermeable walls and, hence $\rho(U_{fluid} - U_{tip}) \to 0$, or equivalently

$$P(U - \alpha\theta) \to 0 \quad \text{as} \quad \theta \to 1 \quad , \tag{21}$$

which implies either a finite fluid velocity $U \to \alpha$ or a full vacuum $P \to 0$ at the leading edge. An important aspect of the present analysis is the identification and resolution of the singularity which must be present if this condition is to be satisfied. To this end, use will be made of the jump-balance [14] relations, derived from first principles or by integrating [12,13] across the jump,

$$[P] = 0 \quad , \quad [P(U - \alpha\theta)] = 0 \tag{22}$$

which, respectively, ensure conservation of momentum (in the degenerate, low M_o sense) and of mass at a singular surface.

IV. EARLY-TIME LAMINAR FLOW STRUCTURE

Already it is known that the fracture grows exponentially during the early laminar-flow period, in accordance with the integral (18) of the time dependent ODE's. But, it remains to determine the separation constant, α in (18). To do that we must calcualte the complete flow field by solving the space dependent (i.e., θ-dependent) ODE's. These solutions are obtained by standard shooting-methods, giving special attention to a singularity at the leading edge of the flow. The asymptotic solution for large N is deduced from a boundary-layer argument.

In laminar flow the integro-differential system (12,13,14,15, 21) can be written in the following form obtained by substituting the equality $U = -P'W^2$ from (13a) into (20) and (21).

$$P(P'W^2)' + (P'W^2 + \alpha\theta)P' = -P((P'W^2 + \alpha\theta)\frac{W'}{W} - \alpha) \quad , \tag{23}$$

$$P(0) = 1 \quad , \quad \lim_{\theta \to 1} P(P'W^2 + \alpha\theta) = 0 \tag{24}$$

$$W(\theta;N) = W(P(\theta);N) \quad , \int_0^1 \frac{P d\theta}{\sqrt{1-\theta^2}} = \frac{\pi}{2N} \quad . \tag{25}$$

The ordinary differential equation (ODE) is second order with a like number of boundary conditions. The separation constant α affords the auxilliary degree of freedom necessary to satisfy the integral constraint.

A singularity is present at an interior point θ^* where in keeping with (22)

$$P(\theta^*) = 0 \ , \quad P'(\theta^*_-) = -\alpha\theta^*/W^2(\theta^*)$$

$$P'(\theta^*_+) = 0 \ . \tag{26}$$

The last ensures that $P(\theta) = 0$ for $\theta^*_- \leq \theta \leq 1$, so that the leading-edge boundary condition (21) is automatically satisfied. The supporting argument outlined below is based on the nature of the ODE as well as the condition that $W'(1) = 0$, and hence $W \sim C\xi^\beta$ ($C = \text{const} > 0$, $\xi = 1 - \theta$, $\beta > 1$) near $\theta = 1$.

(1) It must be that $P(1) = 0$. Otherwise, the boundary condition at $\theta = 1$ requires that $P' \to -\alpha/W^2 \sim -\alpha C^2/\xi^{2\beta}$ with the unacceptable consequence that $P \to -\infty$.

(2) P must vanish at an interior point θ^* so that W'/W has a finite limit from the left. Supposing to the contrary that $P > 0$ as $\theta \to 1$, the ODE requires that $P' \to -PW'/W \sim P/\xi$, and, hence, the contradiction that $P \sim 1/\xi^2$.

(3) $P'_- \to \alpha\theta/W^2$ at θ^*. The ODE admits only two other possibilities; each is discounted: (a) if $P'_- \to 0$, all the higher derivatives also vanish which, on the finite interval, implies that the function is constant to the left of θ^*; (b) if $P' \to \infty$, then $PP'' + P'^2 \to 0$, whereupon $PP' \to C$ in violation of the jump mass-balance (22).

The discontinuity in P' has the character of a degenerate shock. Pressure jump is precluded by the absence of inertial terms at low Mach number. The trailing fluid velocity matches the shock speed, as in a so-called contact interface.

The numerical solution procedure consists of successive iterations of the sequence listed below, starting from the initial

guess that $P(\theta)$ is linear across an entry-layer of thickness $\tilde{\delta}$ (with $\tilde{\delta}$ estimated from (4a)).

(1) Calculate $W(\theta) = W[P(\theta), N]$ from the elastic representation (14) using most-recent $P(\theta)$ in the integrand. Averaging this result with previous $W(\theta)$ affords advantageous damping.

(2) By application of a two-parameter shooting method, solve the problem (23, 24a, 25b, 26) for $P(\theta)$ using most-recent $W(\theta)$ in the ODE. It is elected to regard θ^* and α as shooting parameters (rather than $P'(0)$ and α). Starting with a leftward expansion from guessed θ^*, integration proceeds backward to $\theta = 0$; thereafter checking to see whether $P(0) = 1$ and whether the integral constraint (25b) is met.

(3) Test convergence by checking the agreement between successive interactions.

Standard library routines perform the major operations: simplex minimization iterates the shooting parameters, and a fifth order Runge-Kutta procedure integrates the ODE such that a specified error tolerance (here 10^{-6}) is maintained by adaptive control of the forward step size.

Profiles of pressure and aperture are displayed in Figure 2 for selected values of N. The corresponding data in Table I can be used to estimate the location and velocity of the tip as well as aperture, gas velocity, and mass flow at the entrance. As expected (from (4)) the singular point θ^* shifts backward toward the inlet as N increases. The fracture shape clearly reflects

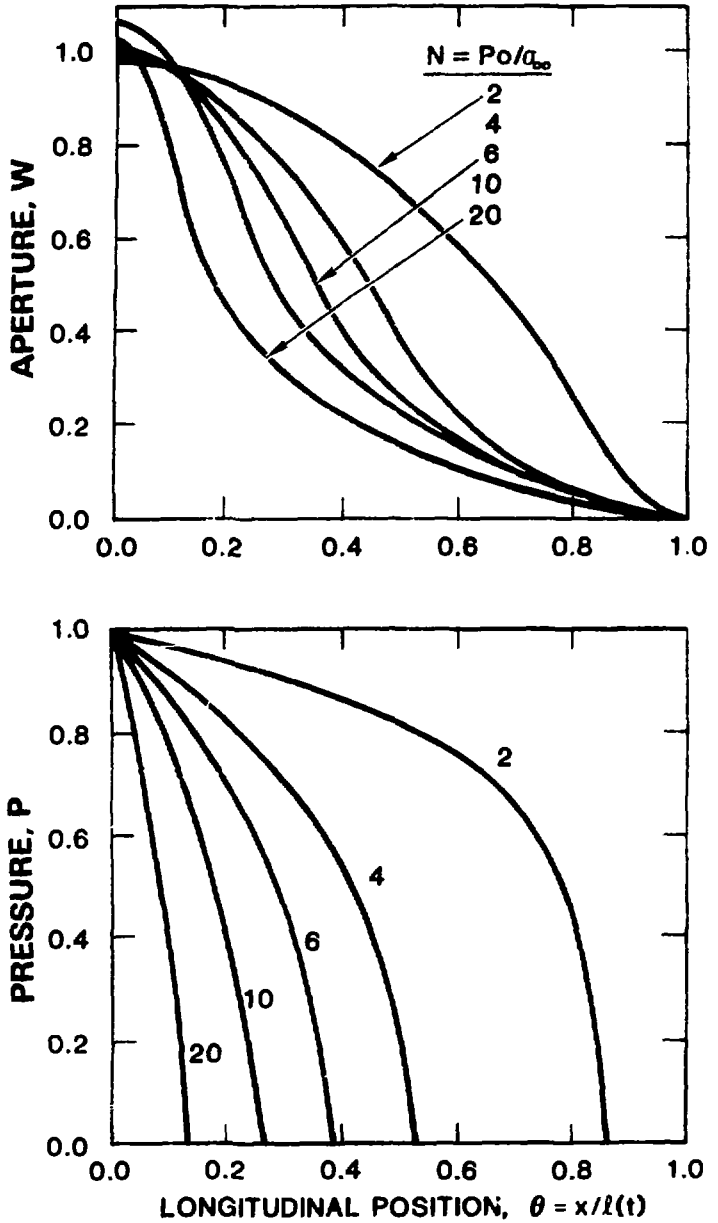

FIGURE 2. Apercure and Pressure Distributions in Laminar Flow

TABLE I

LAMINAR FLOW RESULTS

$N = p_c/\sigma_\infty$	α	θ^*	$W(0)$	$U(0)$
2	0.29	0.86	0.98	0.29
4	1.4	0.54	0.99	0.84
6	3.2	0.40	1.0	1.4
10	9.2	0.27	1.1	2.7
20	38.0	0.13	1.0	5.4
∞	$\left(\frac{N}{\pi}\right)^2$	$\frac{\pi}{N}$	1.0	$\frac{N}{\pi}$

TABLE II

TURBULENT FLOW RESULTS

$N = p_c/\sigma_\infty$	α	$W(0)$	$U(0)$
2	0.73	0.82	0.68
4	2.0	0.95	1.1
6	3.4	1.0	1.5
10	7.3	0.98	1.9
20	21.0	0.98	2.8
∞	$\sim \left(\frac{N}{\pi}\right)^{3/2}$	~ 1.0	$\left(\frac{N}{\pi}\right)^{1/2}$

the extent of the pressurized zone since a discontinuity in W" accompanies the inflection point at η^*. Note that W(1) stays near unity, indicating that the scaling considerations always provide a good estimate (11) of the aspect ratio w_o/ℓ_o. An unexpected feature of the flow is the nearly uniform fluid velocity.

An asymptotic analysis for large N is based on the recognition of growing disparity between the fracture-length and the entry-layer thickness, θ^*. Upon transformation to a boundary-layer coordinate

$$\eta = \theta\sqrt{\alpha} \quad , \tag{27}$$

the ODE no longer depends explicitly on α. For large enough N, (and, hence, large α), it can then be argued that $W = 1$ and $W' \ll 1$ within the entry region, in which case $P(\eta)$ satisfies the following problem (from (23,24a,26)) in which $(\,)' = d(\,)/d\eta$

$$PP'' + P'(P' + \eta) = P \tag{28}$$

$$P(0) = 1$$

$$P(\eta^*) = 0 \ , \quad P'(\eta_-^*) = -\eta^* , \ P'(\eta_+^*) = 0 \ . \tag{29}$$

The piecewise linear solution, which is singular at $\eta^* = 1$,

$$\begin{aligned} P &= 1 - \eta \ , \qquad 0 \leq \eta \leq \eta_-^* \\ P &= 0 \qquad\qquad \eta_+^* \leq \eta \leq \sqrt{\alpha} \end{aligned} \tag{30}$$

is exact in the limit ($N \to \infty$). Substitution of this profile into the integral constraint (25b) shows that $\alpha \to (N/\pi)^2$ as noted in Table I. Convergence to this asymptotic result is demonstrated in Figure 3 where $P(\eta)$ (from the numerical calculations) is plotted for increasing large N.

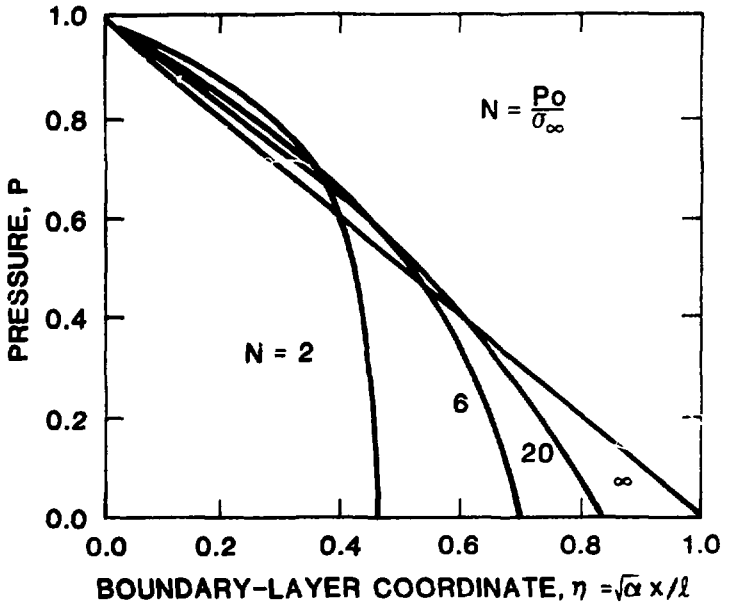

FIGURE 3. Convergence of Laminar Pressure Distribution to The Large-N, Boundary-Layer Solution

V. INTERMEDIATE-TIME TURBULENT FLOW STRUCTURE

The fracture grows like a near-unity power of time during the intermediate turbulent-flow period, in accordance with the integral (18) of the time dependent ODE's. As in the previous laminar-flow regime, it remains to determine the structure of the flow field to calculate the value of the separation constant. The numerical and the asymptotic large-N analyses are essentially the same as before, except that the singularity now lies at the tip of the fracture.

The integro-differential system for a turbulent flow is the same as the laminar case (23-25) except that the previous ODE for P is now replaced by the pair of equations (take $P'/P = -U^2/W^{1+b}$ from (13b) and substitute into (20))

$$U' - (U - \alpha\theta)\,\frac{U^2}{W^{1+b}} = -\left[(U - \alpha\theta)\,\frac{W'}{W} + \alpha\right] \tag{31}$$

$$P = \exp\left[-\int_0^\theta \frac{U^2}{W^{1+b}}\,d\theta\right] . \tag{32}$$

This form is chosen (over the second-order equation for P) because the ODE for U is only first-order and it happens to be independent of P.

The singularity must now lie at the leading edge where in keeping with (21)

$$P \to 0 \quad \text{and} \quad U \to \alpha\theta \quad \text{as} \quad \theta \to 1 \ . \tag{33}$$

There is no other way to satisfy the requirement that $P(U - \alpha\theta) \to 0$, as $\theta \to 1$.

(1) A singularity at an interior point θ^* is strong enough to bring P to zero, but is not strong enough to hold it there. To have $P \to 0$ internally, it is necessary that $U \to \infty$ in which case the ODE requires that $U' \to U^3/W^{1+b}$ ($U^2 \to W^{1+b}/2\xi$, $\xi = \theta - \theta^*$) and hence (using the integral for P) $P(U - \alpha\theta) \to$ constant, so that (by virtue of the jump mass-balance) P cannot be identically zero to the right of θ^*.

(2) It is not possible that $U - \alpha\theta \to \pm\infty$ or that $U - \alpha\theta \to \pm$ constant $\neq 0$ as $\theta \to 1$. This can be verified by local analysis, like that above, with $W \sim (1 - \theta)^\beta$, $\beta > 1$.

The requirement that $U(1) = \alpha$ is the only boundary condition to be satisfied by U.

The numerical calcualtions are easier than in laminar flow, because α is now the only shooting parameter. Expansion from the singularity is followed by a leftward march to the origin, thereafter checking to see if the integral constraint is satisfied. The pressure, P, and the integral constraint, I, are conveniently evaluated by carrying along supplementary ODE's for $(\rho_0 P)'$ and I'. Cyclical alternation between the ODE's and the integral equation is the same as in laminar flow. Results are given in Figure 4 and Table II.

The asymptotic ($N \to \infty$) entrance-layer argument is carried over from laminar to turbulent flow. Upon transformation to the appropriate boundary-layer scaling

$$\hat{\eta} = \theta\alpha^{2/3} \ , \ \hat{U} = U/\alpha^{1/3} \ , \tag{34}$$

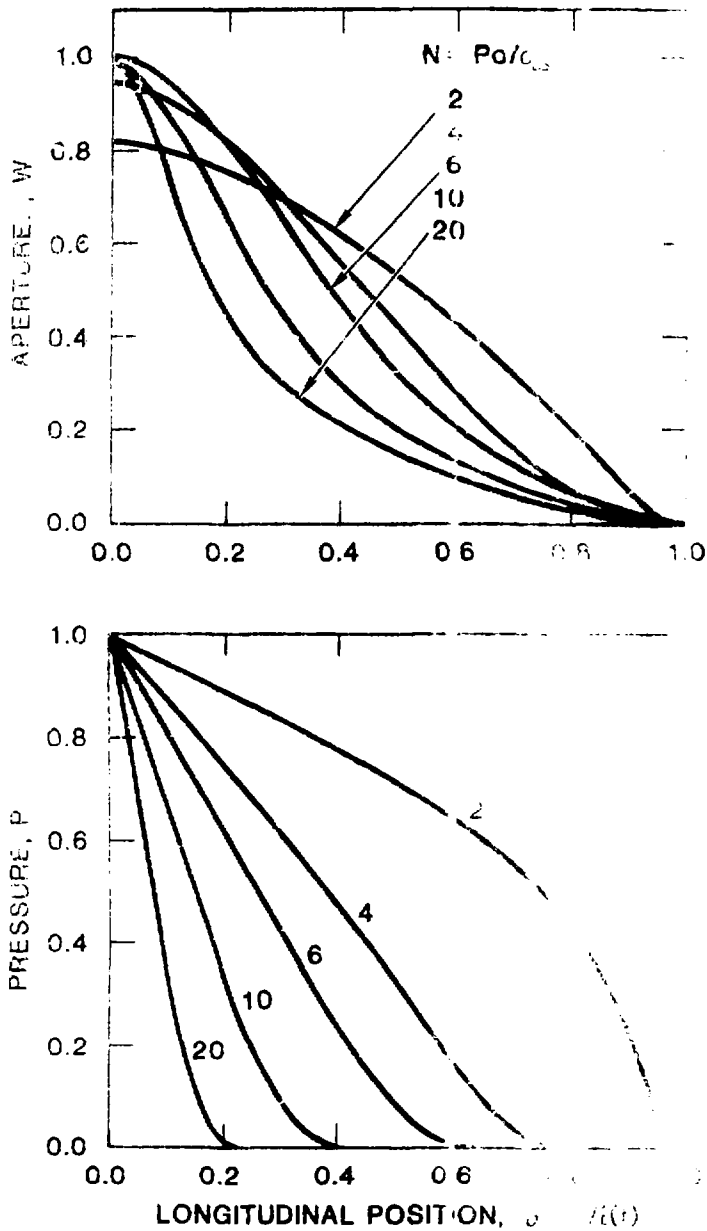

FIGURE 4. Aperture and Pressure Di [illegible] Flow

the inner problem statement ($W = 1$, $W' \ll 1$) is again independent of α (taken from (31,32,33) with $(\ )' = d(\ )/d\hat{\eta}$)

$$\hat{U}' - (\hat{U} - \hat{\eta})\hat{U}^2 = -1 \tag{35}$$

$$P = \exp\left[-\int_0^{\hat{\eta}} \hat{U}^2 d\hat{\eta}\right] \tag{36}$$

$$\hat{U} \to \hat{\eta} \quad \text{as} \quad \hat{\eta} \to \infty \ . \tag{37}$$

The requirement that $\hat{U} \to \hat{\eta}$ ($U \to \alpha\theta$) enforces agreement between the outer behavior of the inner (boundary-layer) solution and the inner behavior (leading terms) of the outer solution (tip expansion) in the spirit of matched asymptotic expansions [15]. By the introduction of a so-called defect-function $\psi = \hat{U} - \hat{\eta}$ which satisfies

$$\psi' - \psi(\psi + \hat{\eta})^2 = -2 \ , \quad \psi(\infty) = 0 \ , \tag{38}$$

it is seen that the boundary condition cannot be satisfied unless $\psi \to 2/\hat{\eta}^2$ as $\hat{\eta} \to \infty$, in which case the ODE is singular at infinity. The computational problem is therefore posed in the independent variable $\xi = \exp(-\hat{\eta})$ in order to bring the singularity to a finite location ($\xi = 0$) from which the local expansion initiates numerical integration toward the entrance ($\xi = 1$). The outcome (for which $\hat{\eta}(0) = 1.1159$) is plotted in Figure 5 where the large-N convergence of $P(\hat{\eta})$ is also presented. The corresponding asymptotic entries in Table II are based on the following observations (from (15b) and examination of Figure 5),

$$\frac{\pi}{2N} = \int_0^1 \frac{P(\theta)\, d\theta}{\sqrt{1 - \theta^2}} \to \alpha^{-2/3} \int_0^\infty P\, d\hat{\eta} \simeq \frac{1}{2}\, \alpha^{-2/3} \ \text{as} \ N \to \infty \ . \tag{39}$$

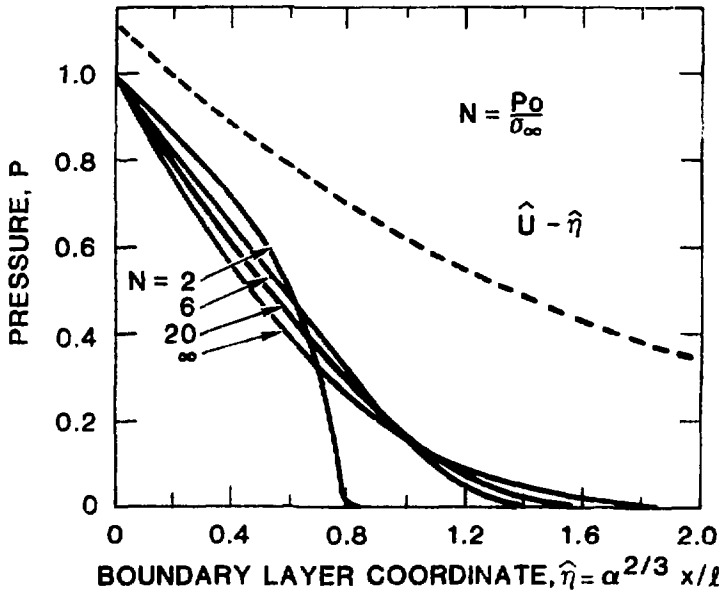

FIGURE 5. Convergence of Turbulent Pressure Distribution To The Large-N, Boundary-Layer Solution (Also Shown is Velocity $\hat{U}$ For $N \to \infty$)

VI. TRANSITIONS

The considered laminar and turbulent flows belong to the class called self-similar asymptotics, each being valid only within a limited window of time. Such asymptotics are often independent of the initial data, as in the initial-boundary value problem for diffusion equations [16]. But, it is not uncommon to find lasting dependence upon the initial data or on an integral measure of the early impetus, as in the spherical propagation of a strong-explosion shock [17] where the late-time asymptotic solution depends upon the initial energy release. The present problem has this latter character throughout the early laminar-dominated period, but it finally becomes independent of the initial data in the late turbulent-dominated period.

The fracture-growth function $g(\tau)$ satisfies a first-order ODE, so it is possible to satisfy only one initial condition at the onset and only one matching condition at each transition. This single constant-of-integration can be interpreted as any extensive measure of the fracture/flow system such as length, volume, or elastic strain energy. It matters little which measure we choose to emphasize since the functional relationships among these integral measures are nearly the same from one asymptotic regime to the next. In this regard, it is recalled that the fracture shape (and, hence, volume and strain-energy) is, for a given pressure ratio N, essentially the same in laminar and turbulent flow, despite the difference in pressure distribution.

The early laminar solution depends linearly upon the (necessarily nonzero) integration constant ℓ_o which characterizes the

the extent of the fracture at the onset of elongation.

(1) Under the supposition of a pre-existing fracture of finite length ℓ_o, it is not difficult to estimate the time required for a pressure wave to penetrate to such a depth (roughly * or †) that elongation begins to occur. During the early stages of this preelongation period, inertial forces may influence the flowfield [2], but viscous forces soon dominate due to the high aspect ratio of a fracture.

(2) As an alternative to a direct specification of ℓ_o, it is apparently sufficient to prescribe the conditions of the unfractured medium (i.e., the reservoir pressure) at incipient breakdown ($t = 0_-$). Knowledge of these conditions can then be used to determine a finite length ℓ_o for which the elastic strain-energy at $t = 0_+$ is the same as the strain-energy at $t = 0_-$.

All that is necessary is that some indication be given of the starting condition from which the gas-drive process initiates.

The flow is not self-similar at breakdown, but is expected to become so in time. The proof that a solution always settles into self-similarity, regardless of initial data, is often prohibitively difficult, but has been given for some representative problems [16,17].

The transition from laminar to turbulent flow (at Re $\approx 2 \times 10^3$) is not long in coming because the Reynolds number ($Re = Re_o fg$) grows exponentially on a very short time scale, $t_o = 12 (\ell_o/w_o)^2 \mu_o \gamma / p_o c_o^2 \ll 1$ s. The integration constant of the

turbulent flow should be chosen so that one of the extensive (integral) measures is continuous at transition. The rate-measures such as g' will, of course, be discontinuous. Aside from the considered case of laminar/turbulent transition during propagation, it is possible (for some prescriptions of data) that the flow could be turbulent at breakdown. The initial or matching conditions for the turbulent flow are not, however, a critical issue since the turbulent solution eventually becomes independent of the initial data.

The dependence upon initial data is qualitatively different in the laminar and turbulent flow regimes. In the laminar solution (from (18a,8,9,16a))

$$\ell = \ell_o \exp\left(\alpha t \left(\frac{w_o}{\ell_o}\right)^2 \frac{c_o^2 \rho_o}{12\mu_o \gamma}\right) \tag{40}$$

there is a lasting dependence on the initial data, ℓ_o. But in the late-time limit of the turbulent solution, which is when it becomes asymptotically valid, (from (18b,8,9,16b) as $\tau \to \infty$)

$$\ell = \left(\frac{2-b}{2} \alpha t \left[\left(\frac{w_o}{\ell_o}\right)^{1+b} \frac{c_o^2}{a\gamma} \left(\frac{1}{\varepsilon}\right)^b\right]^{1/2}\right)^{2/(2-b)} \tag{41}$$

there is no longer any dependence on the initial length scale ℓ_o, since the ratio w_o/ℓ_o is given by (11) in terms of p_o, N and the elastic constants.

The dependence upon initial data is a physical feature of the problem -- not an artifact of the mathematical formulation. The use of asymptotic analysis is, in fact, beneficial in this

respect, because the initial data is distilled into a single constant of integration. This lessens the need for a comprehensive analysis of the initiation process. There has been little previous study of this initiation/propagation coupling because the initial data has no lasting influence if the flow-rate (pumping schedule) is prescribed instead of the driving pressure, as in the oil-field practice of hydrofracture.

The asymptotic solutions for the laminar and turbulent regimes are strictly valid only when the Reynolds number is either very low or very high everywhere within the channel. The transition from laminar to turbulent flow will therefore be a gradual one with turbulence taking over a longer and longer section of the fracture, and there will always be a laminar zone near the tip. The character of such a transition and the validity of the asymptotic solutions have been investigated for the closely related problem of the high-Re to low-Re transitional flow which occurs during transient fluid flow in porous media, or equivalently in narrow capillary tubes or in constant-aperture fractures [18].

VII. SEEPAGE INTERACTIONS IN PERMEABLE MEDIA

If a hydrofracture is driven into a permeable medium, as in the geologic applications, it is important to account for the interactions between the longitudinal flow in the fracture and the induced transverse flow in the surrounding porous medium. This problem has been previously studied for the prototypic case of a constant-aperture fracture and also as a perturbation on the pump-driven hydrofracture problem [1]. In the present application the transport equations for flow in porous media are used to show that seepage interactions become less important as the fracture length increases, and hence the stated self-similar solutions are late-time asymptotics with respect to this consideration.

If a lateral loss-flow with local transverse velocity, v, carries fluid from the fracture into the surrounding medium, the continuity equation for the fracture flow (5a) takes the following modified form

$$\frac{\partial}{\partial t}(\rho w) + \frac{\partial}{\partial x}(\rho w u) = -\rho v \tag{42}$$

but the momentum equation for the fracture remains the same as before (from (5b), dropping the inertial terms for low Mach number)

$$-\frac{1}{\rho}\frac{\partial p}{\partial x} = \frac{1}{\rho}\frac{12\mu u}{w^2} \qquad \text{(laminar)}$$

$$= a\left(\frac{\varepsilon}{w}\right)^b \frac{u^2}{w} \qquad \text{(turbulent)}. \tag{43}$$

To evaluate the seepage velocity, v, it is necessary to consider the surrounding porous-flow field which is governed by the two dimensional continuity equation and by Darcy's Law, respectively,

$$-\phi \frac{\partial \rho}{\partial t} = \nabla \cdot \rho \bar{u} \quad \text{and} \quad \bar{u} = -\frac{\kappa}{\mu} \nabla p \tag{44}$$

which combine to form the composite PDE

$$\phi \frac{\partial \rho}{\partial t} = \frac{\partial}{\partial x}\left(\rho \frac{\kappa}{\mu} \frac{\partial p}{\partial x}\right) + \tag{45}$$

in which ϕ and κ are porosity and [illegible] additional initial condition $p(x,y,0) =$ [illegible] field pressure in the porous medium.

Reconsider now the fracture problem. [illegible] previous similarity transformation [illegible] transverse similarity variable

$$\eta = \left(\frac{\phi \mu}{\kappa P_o}\right)^{\frac{1}{2}} \tag{46}$$

in which y is measured away from [illegible] formed problem statement, including [illegible] follows (where we momentarily [illegible] follows)

$$\theta W P' - \frac{f}{g}(WPU)' + (g'\eta)^{-\frac{1}{2}} \left(\quad W - \theta W' \right) \tag{47}$$

$$\frac{-1}{P} P' = \frac{f^2}{g} b \frac{U^2}{W(1+b)} \quad \text{[illegible]} \tag{48}$$

$$-\frac{1}{2}\eta \frac{\partial P}{\partial \eta} = \frac{\partial}{\partial \eta}\left(P \frac{\partial P}{\partial \eta}\right) + \frac{1}{g^2} \left(\frac{\kappa_o}{\kappa} \right) \tag{49}$$

in which $\theta = 2/(2-b)$ and the new [illegible] parameter, R, is defined as

$$R = \frac{1}{u_o} \left(\frac{P_o \phi \kappa}{\mu_o W_o} \right) \quad \frac{\text{[illegible]}}{\text{[illegible]}} \tag{50}$$

and for simplicity it has been assumed that the interstitial fluid is the same as the fracture fluid, say air. The porous diffusion equation (49) is indicative of a boundary-layer structure in which longitudinal diffusion is negligible, particularly at late times when $\tau/g^2 < 1$. From previous solutions of this diffusion equation (49) for constant-aperture fractures [19], it is known that $\partial P/\partial \eta$ is of order 1 along the fracture surface, and hence $\partial P/\partial \eta$ is of order 1 in equation (47).

The question is, under what limit (early or late) does the seepage term make a negligible contribution contribution to the fracture-flow continuity equation (47)? In that limit (be it early or late) the fracture growth rate will revert to the form given previously

$$g \sim \tau^{\lambda} \qquad (\lambda > 1) \qquad \text{(turbulent)} \tag{51}$$

Thus, the limiting condition of negligible seepage must occur as $\tau \to \infty$, because in that limit

$$\frac{1}{g^{1}\sqrt{\tau}} \sim \frac{1}{\tau^{(\lambda-1)}\sqrt{\tau}} \to 0 \quad \text{(turbulent)} \tag{52}$$

and hence the seepage term becomes negligible in (47). In order for seepage losses to diminish as time increases, it is only necessary that $\lambda = 2/(2-b)$ be greater than 1. Typically $b = 1/2$ and $\lambda = 3/2$ in turbulent flow, and in laminar flow the exponential growth is stronger than any power of time (i.e., $\lambda \to \infty$). Thus, seepage losses should always become negligible at late times, either in laminar or in turbulent flow.

Physically, the seepage interaction diminishs at late times, because an increase in aperture, w, enhances the longitudinal through-flow more than the corresponding increase in length, ℓ enhances the seepage losses (i.e., enhances the surface area for seepage loss). This would not be the case if the fracture aperture were held constant during extension or if the geometry were axi-symmetric and, hence, the loss area were increasing in proportion to ℓ^2, instead of ℓ.

Although the impermeable-medium results must be regarded as late-time asymptotics for the permeable case, and the seepage interactions will always result in a finite tip-pressure, the zero-pressure impermeable analysis should be a good approximation so long as the pressure ratio, $P_{driving}/P_{tip}$, is large (say, 5 or more) as observed for the closely related problem of transient flow through porous media or in slender channels [18].

VIII. SUMMARY

A problem of gas-driven fracture propagation has been solved by separation of the time and position variables, followed by numerical integration of the resulting ordinary differential equations. The considered case is a prototypic one, subject to a number of simplifications: the elastic field is symmetric and two-dimensional, the ideal-gas fow is one-dimensional and isothermal, the driving pressure p_o is constant, and the fractured medium is linearly-elastic, impermeable, and in uniform compression σ_{∞} at infinity.

In the formulation and analysis of such a rudimentary problem, there has been little mention of the many complications which may accompany gas-driven fracture: three-dimensionality, seepage losses in porous media, and energy transfer mechanisms which are particularly prominent in two-phase, steam-driven, nuclear applications. Such interactions must ultimately be integrated in the general and comprehensive context of code development, as exemplified by the pioneering work of Pitts and Brandt [2] and Keller, Davis, and Stewart [3]. The complementary purpose of rudimentary analyses is to: isolate important aspects; gain qualitative understanding; identify mathematical and numerical difficulties associated with boundary layers, singularities, and untractable boundary conditions; and to provide fundamental quantitative results for estimation purposes and as a validation tool in more advanced code development.

The prototypic problem of gas-driven fracture reveals a number of interesting and perhaps unexpected features of the fluid/solid system response

(1) The flow accelerates through a sequence a self-similar asymptotic regimes: laminar, turbulent, and inviscid; only the first two are reported here.

(2) A strong vacuum exists at the tip of the fracture, either in an impermeable medium or in a permeable medium at late times.

(3) The flow effectively experiences a diverging/converging channel, because of the competing effects of time-wise wall divergence, $\partial w/\partial t$, and space-wise wall convergence, $\partial w/\partial x$.

(4) If the pressure ratio ($N = P_o/$) is large, the flow is confined to a narrow entry-layer region at the entrance to the channel.

(5) In laminar-dominated flow at early times: the fracture grows exponentially, the pressure goes to zero at mid-span, and the pressure distribution is linear for large values of N.

(6) In turbulent-dominated flow at late times: the fracture grows like a near-unity power of time, the pressure goes to zero at the tip, and the pressure distribution is exponential for large values of time.

(7) The initial data (i.e., length $_o$ at the onset of gas-drive) has a lasting influence in the early laminar period but not in the late-time limit of the turbulent period.

Assumptions and approximations in the analysis are self-consistent with respect to two different criteria: late-time, long-fracture limit (quasisteady stress field, impermeable media, no tensile strength); and upper-bound on fracture extension (all above, isothermal in spite of work done, wedge-shaped configuration).

Quantitative results provide convenient estimates of fracture propagation rates and other engineering data.

(1) Temporal variation of length, aperture and velocity is described by the analytic expressions

$$\ell = \ell_o g(\tau),\ w(0,t) = w_o W(0) g(\tau),\ u(0,t) = u_o U(0) f(\tau)$$

in which: $g(\tau)$ and $f(\tau)$ are given by (16,17); $\tau = t/t_o$ and $t_o = \ell_o/u_o$; ℓ_o is the initial fracture length; w_o and u_o are defined in (9) and (15); and Tables I and II provide α, $W(0)$, and $U(0)$ as functions of N. See in particular equations (40,41) for $\ell(t)$.

(2) Spatial variations in pressure, aperture, and velocity are presented graphically.

(3) Asymptotic results for large N are particularly simple and, by demonstrating convergence, they lend verification to the numerics.

The dependence upon physical constants, process parameters, and initial data is clear, particularly as N becomes asymptotically large.

IX. REFERENCES

1. G. C. Howard and C. R. Fast, Hydraulic Fracturing, Society of Petroleum Engineers of AIME, Dallas, 1970.

2. J. H. Pitts and H. Brandt, "Gas Flow in a Permeable Earth Formation Containing a Crack," Journal of Applied Mechanics 44, pp. 553-558 (1977).

3. C. E. Keller, A. H. Davis, and J. N. Stewart, "The Calculation of Steam Flow and Hydraulic Fracturing in a Porous Medium with the KRAK Code," Los Alamos Scientific Laboratory Report LA-5602-MS, 1974.

4. R. P. Nordgren, "Propagation of Vertical Hydraulic Fracture," Society of Petroleum Engineers Journal 12, pp. 306-314 (August 1972).

5. A. A. Daneshy, "On the Design of Vertical Hydraulic Fractures," Journal of Petroleum Technology 25, pp. 83-97 (January 1973).

6. A. H. England and A. E. Green, "Some Two-Dimensional Punch and Crack Problems in Classical Elasticity," Proc. Cambridge Phil. Soc. 59, pp. 489-500 (1963).

7. J. Geertsma and F. De Klerk, "A Rapid Method of Predicting Width and Extent of Hydraulically Induced Fractures," Journal of Petroleum Technology 21, pp. 1571-1581 (December 1969).

8. G. I. Barenblatt, "The Mathematical Theory of Equilibrium Cracks in Brittle Fracture, "Advances in Applied Mechanics 7, pp. 55-129 (1962).

9. H. Abe', T. Mura, and L. M. Keer, "Growth Rate of a Penny-Shaped Crack in Hydraulic Fracturing of Rocks," Journal of Geophysical Research 81, (29), pp. 5335-5340 (1976).

10. T. K. Perkins and W. W. Krech, "The Energy Balance Concept of Hydraulic Fracturing," Society of Petroleum Engineers Journal 8, pp. 1-12 (March 1968).

11. A. H. Shapiro, The Dynamics and Thermodynamics of Compressible Fluid Flow, II, Ronald Press, New York (1954).

12. A. Clemins, "Modified Governing Equations for Unsteady Compressible Flow in Ducts," Journal of Applied Mechanics 45, pp. 723-726 (1978).

13. J. L. Huitt, "Fluid Flow in Simulated Fractures," AICHE Journal 2, (2), pp. 259-264 (1956).

14. J. C. Slattery, Momentum, Energy, and Mass Transfer in Continua, McGraw-Hill, New York (1972).

15. J. D. Cole, Perturbation Methods in Applied Mathematics, Blaisdell, Waltham, Massachusetts (1966).

16. G. H. Pimbley, Jr., "Wave Solutions Traveling Along Quadratic Paths for the Equation $u_t - (k(u)u_x)_x = 0$," Quarterly of Applied Mathematics, XXXVII (1), pp. 129-138 (1977).

17. G. I. Barenblatt and Ya. B. Zel'dovich, "Self-Similar Solutions as Intermediate Asymptotics," Annual Review of Fluid Mechanics 4, pp. 285-312 (1972).

18. R. H. Nilson, "Transient Fluid Flow in Porous Media: Inertia-Dominated to Viscous-Dominated Transition," SAND80-0453, Sandia National Laboratories, Albuquerque, NM (1980), J. Fluids Eng. 103 (2), pp. 339-343 (1981).

19. R. H. Nilson, "Transient Two-Dimensional Diffusion Along A High-Diffusivity Lamina Which Bisects a Half-Space", J. Eng. Math. 14 (4), pp. 263-282 (1980).